

Analysis of 258 Different Lesions of the Central Nervous System for Real Time Histopathological Diagnosis Using Confocal Laser Endomicroscopy

Samira Daali^{1*}, Mehreen Javed,¹ Ann-Kristin Altekoester¹, Maximilian Linxweiler², Richard Bostelmann³, Juergen Schlegel⁴, Alhadi Igressa^{5#}, Patra Charalampaki^{5#}

¹Department of Neurosurgery, Hospital Merheim, Cologne Medical Center, Germany

²Department of Otorhinolaryngology, Saarland University Medical Center, Saarland University, Germany

³Department of Neurosurgery, Heinrich Heine University Düsseldorf, Düsseldorf, Germany

⁴Department of Neuropathology, Technical University Munich, Munich, Germany

⁵Department of Neurosurgery, Hospital Merheim, Cologne Medical Center, Germany

#contributed equally

Abstract

Objective: The safe removal of central nervous system tumors in or near eloquent tissue remains extremely challenging due to its complex anatomy. The injury of eloquent tissue can have serious consequences for both mental and physical health while an insufficiently resected tumor bears a high risk of tumor recurrence decreasing the patient's life quality and quantity. The novel method, confocal laser endomicroscopy (CLE), promises safe tumor resection as it permits intraoperative histological imaging of tissues in real-time. Thus, aim of the current study was to evaluate CLE for a fast diagnosis of brain and spinal cord lesions in neurosurgery.

Methods: CLE was used for an *ex vivo* assessment of tumor samples from 258 diverse central nervous system lesions. Additionally, traditional histology was performed on the same examined tissue as the gold standard. Non-neoplastic brain tissue served as a control.

Results: The examination of brain and spinal biopsies using CLE allowed the identification of healthy tissue, primary brain and spinal tumors, metastases, abscesses and vascular malformations with a high accuracy of 88.64%. Confocal imaging provided precise cellular and sub-cellular details such as psammoma bodies in meningiomas, perivascular pseudorosettes in ependymomas, microvascular proliferation in glioblastomas and mitotic activity in high-grade tumors.

Conclusion: CLE is a promising method for distinguishing tumor from the surrounding healthy tissue, as well as for the immediate diagnosis of biopsies. Our studies have the potential to establish a faster preliminary diagnosis in an ongoing surgery as compared to current available methods. Moreover, the presented characteristic cellular and subcellular confocal features of examined tumors and non-neoplastic tissues could be used to guide future tumor surgeries to enable a more precise and safe resection.

Keywords: Confocal laser end microscopy; Neurosurgery; Neuropathology; Brain tumor; Spinal tumor; Acriflavine hydrochloride

Introduction

Surgery, chemotherapy, and radiation therapy are the most common procedures to treat brain and spinal cord lesions depending on the World Health Organization (WHO) classification and definition [1]. Surgery is used to identify abnormal tissues histologically, to determine how far a tumor has spread and finally to remove the tumor. In neurosurgery, various techniques have been established to guide tumor resection such as fluorescence-guided surgery, intraoperative magnetic resonance imaging (MRI), neuronavigation and ultrasonography. None of these techniques are able to distinguish tumor from healthy tissue at a cellular level, which is essential to accomplish a complete resection of the tumor without injuring healthy surrounding tissue. An incomplete resection of a tumor results in a higher risk of tumor recurrence, decreased life quality and a shortened lifetime [2]. Currently, traditional histopathology is routinely performed to establish diagnoses, but it is very time-consuming and therefore not ideally suited to assist surgery. Frozen section analysis is currently the fastest intraoperative method for preliminary tumor diagnosis and assessment of tumor margins [3]. Unfortunately, this method bears several shortcomings, such as the occurrence of freezing artifacts, sampling errors and a poor sample quality. Hence, new histopathological methods are required to improve the diagnostic yield of biopsies during tumor resections. Confocal laser endomicroscopy (CLE) is such a promising method as it achieves *in vivo* histologic imaging at a 1000-fold magnification in real-time without special tissue manipulation [4]. Furthermore, the compact size

and maneuverability makes the CLE device suitable for routine use in surgery. In 2004, CLE was first used in gastroenterology to perform optical biopsies [4]. Since then, it has been introduced into urology, gynecology, otolaryngology and pulmonology for tumor diagnosis [4-10]. Surprisingly, experience with CLE in neuro-oncology is mainly limited to studies on animal models and less on human samples [11-16]. CLE would represent an excellent tool in the challenging surgery of central nervous system (CNS) tumors since due to this real-time diagnosis healthy vital tissue would be more easily distinguishable and could therefore avoid a second surgery. To achieve this goal, the neurosurgeon and/or neuropathologist would require a basic knowledge of the tumor cytoarchitecture imaged by CLE.

Thus, aim of this study was to examine various pathological brain and spinal cord biopsies *ex vivo* in order to define diagnostic confocal features using traditional histopathology as the gold standard. We

***Corresponding author:** Mrs. Samira Daali, Department of Neurosurgery, Cologne Medical Center, Ostmerheimerstr. 200, 51103 Cologne, Germany; Tel.: +49 1729550615; Fax: +49-221-8907-13373; E-mail: Samiradaali4@gmail.com

Received February 19, 2016; **Accepted** March 31, 2016; **Published** April 07, 2016

Citation: Samira D, Mehreen J, Ann-Kristin A, Alhadi I, Maximilian L, et al. (2016) Analysis of 258 Different Lesions of the Central Nervous System for Real Time Histopathological Diagnosis Using Confocal Laser Endomicroscopy. J Mult Scler (Foster City) 3:169. doi:10.4172/2376-0389.1000169

Copyright: © 2016 Samira D, et al. This is an open-access article distributed under the terms of the Creative Commons Attribution License, which permits unrestricted use, distribution, and reproduction in any medium, provided the original author and source are credited.

analyzed clinical features on 258 cases of astrocytoma grades I-IV, choroid plexus papillomas, meningiomas, hemangioblastomas, epidermoid cysts, schwannomas, plasmacytomas, cavernomas, ependymomas, pituitary adenomas, metastases, abscesses and other, more seldom entities. Further, we analyzed histopathological features of non-neoplastic tissue as a control and calculated the accuracy of correct diagnosis. To the best of our knowledge, this collection of neuro-lesions examined by CLE is the largest described to date. It represents a first guideline for neuropathologists and surgeons to interpret *ex vivo* as well as *in vivo* CLE images of human tissues in real-time.

Materials and Methods

Technical considerations

For the examination of human brain and spinal cord lesions the confocal laser endomicroscopic system Cellvizio[®] (Mauna Kea Technologies, Paris, France) was used. The Cellvizio[®] system consists of a blue laser scanning unit (LSU-488), imaging mini-optical probes, and the software. The micro mini-optical probes of the Cellvizio[®] system are composed of thirty-thousand optical fibers and are available for various clinical purposes (Gastroflex[™], GastroFlex[™] UHD, ColoFlex[™], ColoFlex[™] UHD, CholangioFlex[™], UroFlex[™], CystoFlex[™], AQ-Flex[™] 19, CystoFlex[™] UHD; Mauna Kea Technologies, Paris, France). They can be passed down the accessory channel of any standard endoscope.

In this study the Gastroflex[™] probe, which is 3 m long and has an internal diameter of > 2.8 mm, was used for examination. The confocal image field of view is Ø 240 µm with a lateral resolution of 1 µm and an imaging plane depth of 55-65 µm. The blue laser uses an excitation wavelength of 488 nm and a light emission detector of 500-650 nm. A 4-kHz oscillating mirror and a galvanometric mirror managed real-time imaging for horizontal scanning and frame scanning, respectively. The resulting frame was 12 Hz and the spatial resolution 2-5 µm. After a two-step calibration, the Cellvizio[®] system was ready to use. The Cellvizio[®] software unit supports the export and modification of the videos.

Collection and confocal imaging of human tissues

Pathological biopsies were collected from 258 patients that had undergone surgery at the Department of Neurosurgery in the Merheim Hospital (Table 1). All procedures involving human participants were performed in accordance with the ethical standards of the institutional and/or national research committee as well as the 1964 Helsinki declaration and its later amendments or comparable ethical standards.

Confocal imaging was performed by applying the probe directly to the tissue and recording the images as video sequences. Specimens were first examined natively (prior to staining) and then following staining with 1 drop of 0.01 mg/ml AF (Sigma Aldrich, Melbourne, Australia) dissolved in saline, which primarily stains the nuclei and to a minor extend the cell membrane and the extracellular matrix. After an incubation time of 1 minute, the tissues were washed with saline. CLE images for each patient were exported and stored in a specified folder. The specimens were stored in 4% formalin.

Histopathology

Specimens were fixed in formalin, embedded in paraffin (FFPE) and processed for histopathology at the division of Neuropathology Technical University of Munich. The slides were stained with hematoxylin and eosin (HE) according to standard protocols.

Statistical Analysis

A statistical analysis of the confocal images was carried out in order

Pathological diagnosis	Number of samples
I. Tumors of neuroepithelial tissue	62
Astrocytoma WHO grade I-III	9
Glioblastoma	43
Oligodendroglioma	3
Ependymoma	5
Choroid plexus papilloma	2
II. Tumors of cranial and paraspinal nerves	13
Schwannoma (neurinoma)	11
Neurofibroma	2
III. Tumors of the meninges	81
Meningioma	74
Cavernoma (Haemangioma)	2
Lipoma	2
Liposarcoma	1
Hemangioblastoma	2
IV. Tumors of the haematopoetic system	5
Plasmacytoma	5
V. tumors of the sella region	15
Pituitary adenoma	13
Craniopharyngioma	2
VI. Metastatic tumors	69
Brain metastasis of bronchial carcinoma	46
Brain metastasis of mamma carcinoma	10
Brain metastasis of prostata carcinoma	8
Brain metastasis of rectum carcinoma	5
VII. Cysts and tumor-like lesions	13
Abscess	3
Aneurysm	8
Cyst	1
Epidermoid	1

Table 1: Origin and number of human tumor samples examined by CLE.

to establish the accuracy of CLE. Images of n=258 different human tissues were evaluated by n=4 different evaluators (surgeons and neuropathologists). The traditional histopathological findings, which are the gold standard, were blinded to both groups.

Results

The WHO grading scheme [1,17] was used to interpret cell features of different CNS lesions (n=258) visualized by CLE. We applied topical AF for fast, immediate *ex vivo* tumor staining. AF stained predominately the cell nuclei and to a lesser amount the cell membrane. CLE images showed similar features as compared to HE-stained sections of the same tissue. Below we describe some examples from primary brain and spinal tumors, metastases, abscesses and more seldom CNS lesions in comparison to healthy tissue. A summary of all the examined biopsies can be found in Table 1.

Healthy cortex tissue

Histological as well as during CLE imaging we could differentiate between neurons, oligodendroglia and astrocytic cells. Astrocytes had a round to oval nucleus with open chromatin and peripheral nucleoli. The cytoplasm was branched. Oligodendrocytes were small round cells with dispersed nuclear chromatin. Neurons had a large nuclei and prominent nucleoli. Healthy tissue was easy to identify due to a clear cell structure and arrangement while neoplastic tissue had usually larger nuclei varying wildly in shape and amount (Figure 1).

Astrocytoma WHO grades I-III

Nine astrocytomas were examined, including four pilocytic astrocytomas (WHO grade I), three diffuse astrocytomas (WHO grade II) and four anaplastic astrocytomas (WHO grade III).

CLE images of the pilocytic astrocytomas showed detailed features such as bipolar cells with elongated “hairlike” processes arranged in bundles. Furthermore, we observed Rosenthal fibers, cysts and calcifications, consistent with matched HE-stained section. No mitotic

figures or necrosis were detected as compared to higher-grade astrocytic tumors. In CLE images of anaplastic astrocytomas, an increased cell density, diffusely distributed atypical cells and nuclear pleomorphism were clearly visible.

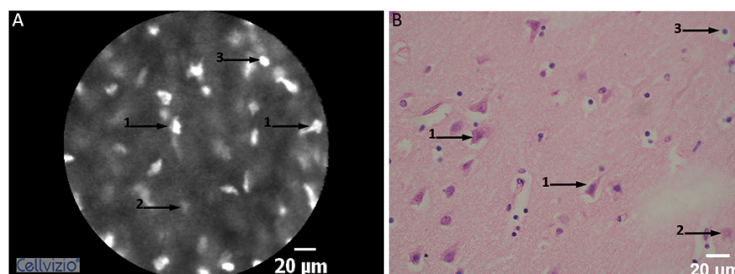


Figure 1: Non-neoplastic cortex tissue. Confocal and histological examination of non-neoplastic cortex tissue revealed neurons, oligodendroglia and astrocytes cells. Non-neoplastic tissue was easy to identify due to a clear tissue and cellular arrangement. Bars = 20 µm.

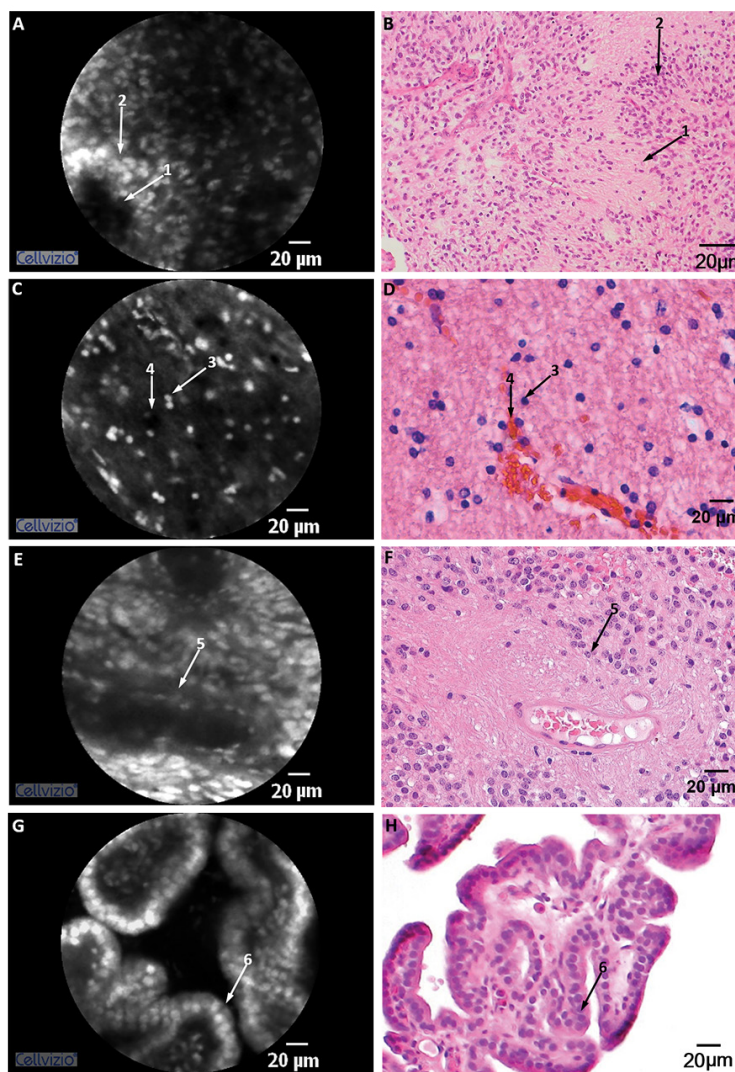


Figure 2: Confocal images (left) and corresponding histopathological sections (right) of neuroepithelial tumors. Analysis of glioblastoma (A, B) showed a high cell density of pleomorphic tumor cells. Necrosis (1→) surrounded by pseudopalisading (2→) are clearly visible on both modalities. Round, uniform nuclei (3→) were typical features of all examined oligodendrogliomas (C, D). Vascular proliferation (4→) was found especially in grade III tumors. On ependymoma II CLE images (E) as well as on the corresponding HE staining (F) perivascular pseudorosettes were a common feature (5→). Imaging of choroid plexus papilloma as well as histological evaluation showed crypt structures with a flat layer of epithelial cells surrounding the fibrovascular cores (6→). Bars = 20 µm.

Glioblastoma multiforme (GBM)

In all of the examined 43 GBMs, regions with high cell density and frequent necrosis were identified via CLE and HE staining (Figure 2 A,B). Necrosis was found both with and without pseudopalisades (accumulation of tumor cells around central necrosis). Vascular proliferation was increased, but vessels could not be specifically identified as glomeruloid or “endothelial proliferation”. Furthermore, pleomorphism, anaplasia and anisokaryosis were detected in the cells. The nuclear to cytoplasmic ratio was increased, the cells were mainly spindle shaped and the nuclei oval or elongated. In a few nuclei multiple, distinct nucleoli were detected. Mitoses and apoptosis were hardly visible while in traditional histology a few were detected.

Oligodendroglioma

We examined three anaplastic oligodendrogliomas of WHO grade III. Characteristic features were round, uniform nuclei and nucleoli, which were clearly visible on both image modalities (Figure 2 C,D). Vascular proliferation was observed in all three examined grade III tumors using CLE. Mitotic activity was assumed to be present in some tumors.

Ependymoma

Four ependymomas (WHO grade II) were examined using CLE. We analyzed perivascular pseudorosettes, which were shown in transversal as well as in longitudinal orientation on CLE images but only in transversal on histology (Figure 2 E,F). Moreover, we detected a moderate cell density, small oval nuclei, microvascular proliferation and necrosis on confocal images comparable to findings of traditional histology.

Choroid plexus papilloma

Two choroid plexus papilloma specimens were compared to traditional histology. Confocal images as well as traditional histology showed crypt structures with ordered, flat epithelial cells around fibrovascular cores (Figure 2 G,H). Cytological atypia, mitosis or necrosis was detected neither on CLE images nor on histology images.

Schwannoma

Nine schwannomas WHO grade I and two schwannomas WHO

grade II were analyzed. Confocal imaging illustrated spindle cells with indistinct cytoplasm. Furthermore, Schwann cells with highly ordered cellular components called “Antoni A” areas (Figure 3 A,B) with Verocay bodies and “Antoni B” pattern with a looser stroma and fewer cells were identified. In HE-sections large and thick walled blood vessels were observed in “Antoni B” areas.

Neurofibroma

The tumor was characterized by a low to medium cell density on traditional histology as well as on confocal images (Figure 3 C,D). The Schwann cells had elongated, curved nuclei without prominent nucleoli. No mitotic activity was detected.

Pituitary adenoma

Thirteen biopsy samples of WHO grade I pituitary adenomas were examined. Using CLE imaging, typical histopathological features such as a monomorph cellular appearance, and dense, round to ovoid nuclei were displayed. Compared to non-neoplastic brain tissue, these benign tumors showed a higher cellular density. On CLE images, cells arranged in clumps surrounded by a cell free layer were detected (Figure 4 A,B). Mitoses and atypia were absent.

Meningioma

Seventy-five meningiomas, forty-nine of which were WHO grade I, were examined using CLE. Analysis of meningiomas grade I resulted in histological features that corresponded to those on HE-sections (Figure 4 C,D). Confocal images showed psammoma bodies, which were characteristic to their histological subtype. Psammoma bodies were observed as round, anuclear structures. Meningiomas grade II of clear cell meningiomas exhibited uniform, round cells and cytological blandness. Furthermore, this tumor type had low-level mitotic activity, and no psammoma bodies. Compared to meningiomas grade I, meningiomas grade II showed an increased cellularity, a higher nuclear to cytoplasmic ratio and more mitotic figures. Three WHO grade III meningiomas were examined. On HE-sections, this type showed several atypical features such as increased mitotic activity and anaplasia. However, such features were difficult to identify on confocal images.

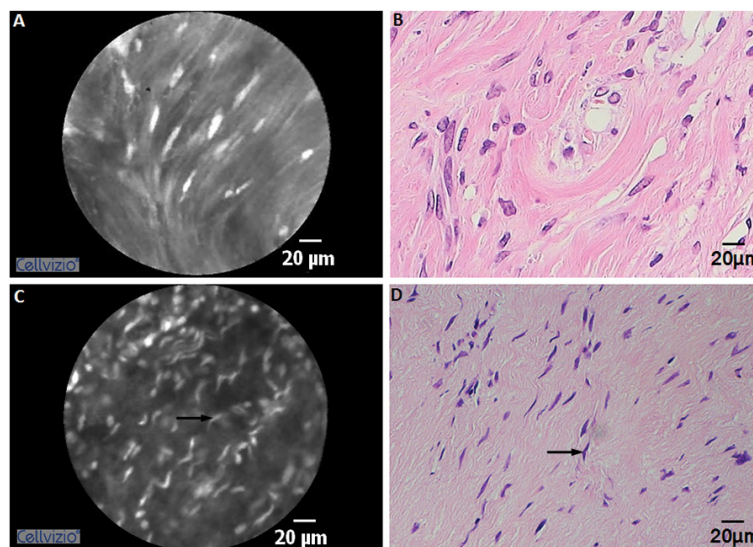


Figure 3: Confocal (A, C) and histological (B, D) analysis of cranial and paraspinal nerve tumors. Imaging of a schwannoma showed compact spindle Schwann cells of an Antoni A tissue (A, B). Schwann cells of neurofibroma (C, D) had elongated, curved nuclei without prominent nucleoli on both imaging methods (→). Bars = 20 µm.

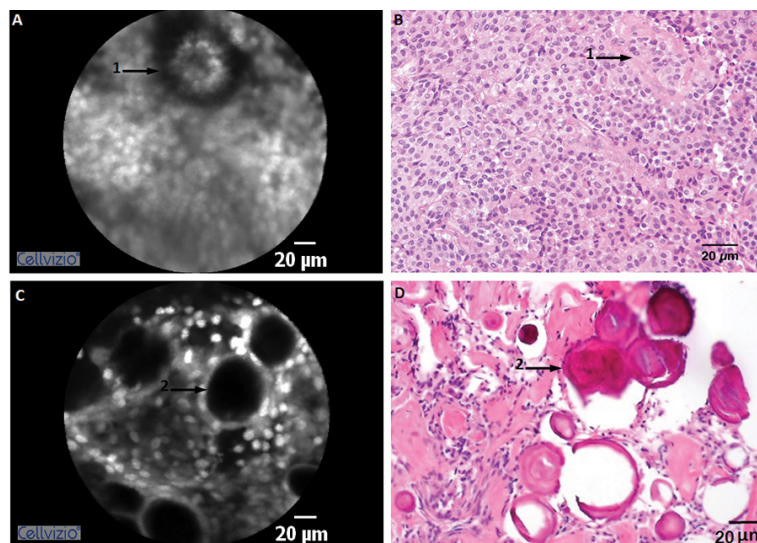


Figure 4: Confocal and HE staining of a meningioma and pituitary adenoma specimen. On pituitary adenoma WHO grade I images (A, B), the monomorph cell appearance as well as the cells arranged in clumps surrounded by a cell free layer were clearly visible (1→). The macronodular pattern of the adenoma is unusual (A). Both HE and confocal imaging of the meningioma specimen showed psammoma bodies as round, anuclear structures (2→). Metaplasia, a common feature of psammoma body-rich meningiomas, is observed on HE stained section (D). Bars = 20 μ m.

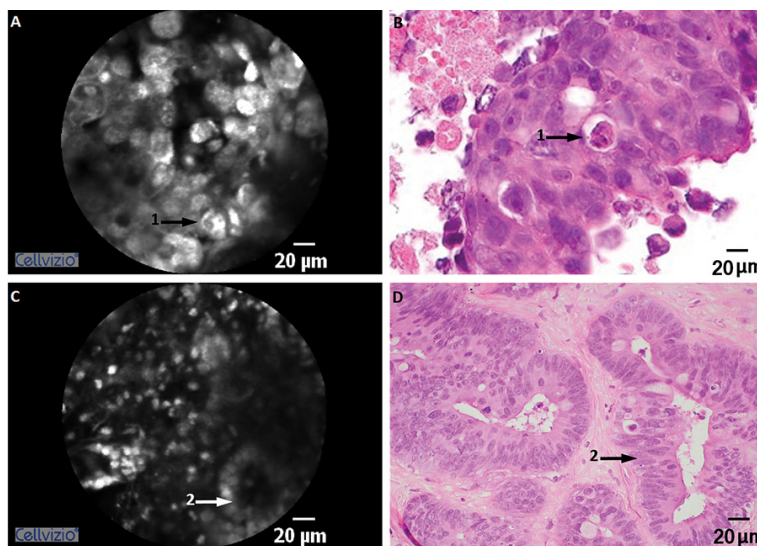


Figure 5: Analysis of adenocarcinoma of the lung and rectum. Confocal images and the corresponding HE staining's of metastasis rectum (C, D) and non-small cell lung carcinoma (A, B). Glandular structures were detected in the metastasis rectum specimen using CLE (C2→). High cell density with a round-to-fusiform shape and big nucleus were a common feature in non-small cell lung carcinoma (A1→). Bars = 20 μ m.

CNS metastasis from adenocarcinoma

The most frequent metastasis in our collection was adenocarcinoma from the lung (n=46). High cell density with a round-to-fusiform shape and big nucleus were a common feature in non-small cell lung carcinoma (Figure 5 A,B). Metastases from the rectum were rare in our collection (n=2). Glandular structures were observed in all adenocarcinoma specimens using CLE and were comparable to HE-sections (Figure 5 C,D). Furthermore, cells with large nuclei and prominent nucleoli as well as mitotic activity were detected in rectum carcinoma. Tissue examination of brain metastasis from mamma carcinoma revealed a lawn-like, partly nester-like growth pattern between a focal distinctive, highly fibrotic stromal component. Moreover, extensive mixed-cell and leukocytic infiltrates were observed.

Small cell lung carcinomas

Metastatic small cell carcinomas from the lung displayed small cells with a round-to-fusiform shape and high mitotic activity on confocal images. No prominent nucleoli were observed. Furthermore, extensive necrosis was present. In HE-stained sections, the tumor cells appeared as a monotonous population that had a very "blue" appearance due to the lack of cytoplasm in the cells.

Epidermoid cyst

Confocal imaging revealed the anuclear keratinizing squamous epithelium as well as the lower layers of the epidermis (Figure 6). The granular layer appeared especially bright due to the high amount of stained nuclei by AF. CLE analysis showed neither calcification nor mitosis.

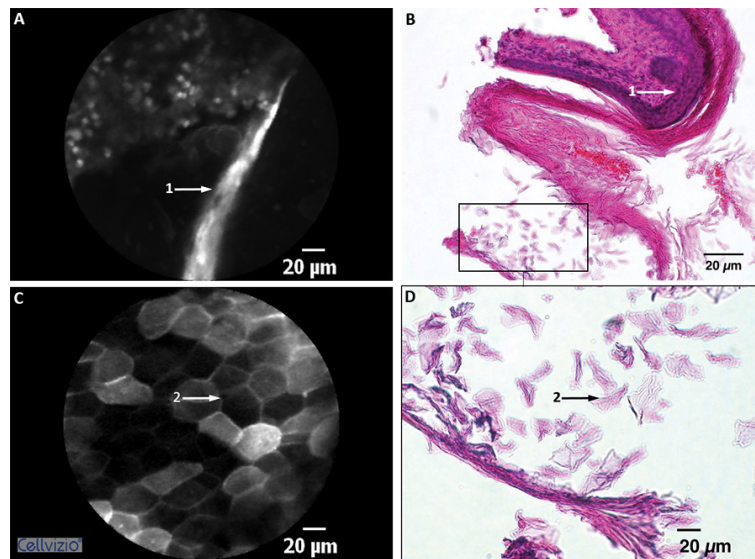


Figure 6: Comparison of HE (C, D) stained and confocal endomicroscopic images (A, B) of an epidermoid cyst. The nucleolar squames are visualized in detail using CLE, while in traditional histology the “ghost cells” are detached from the epithelium (2→). (A1→): Granular layer of the epithelium is very bright due to the high content of stained nuclei by AF. Bars = 20 µm.

Hemangioblastoma

Two biopsy samples of WHO grade I hemangioblastoma were analyzed. Confocal images showed similar features to corresponding HE-stained sections. Prominent vasculature and stromal cells including vacuoles were common features. Nuclear pleomorphism and nucleoli were also evident, whereas mitosis was absent.

Plasmacytoma

We examined five WHO grade I plasmacytomas using CLE. We observed a high cell density, a high number of blood vessels, and pleomorphism.

Cavernoma

Two cavernomas were imaged using CLE. Beside high cell density and pleomorphism, high vascular malformations and spaces were identified (Figure 7).

Abscess

Abscesses examined using CLE showed a characteristic necrotic, purulent center. The center was surrounded by a high cell density of mononuclear cells, astrocytes and other cell types.

Additionally, specific cellular features of other lesions, including bronchial carcinoma, prostata carcinoma, lipoma, liposarcoma, neurofibroma, osteolysis, pharyngioma, and aneurysm were also identified and were consistent with the histology of the same tissue (data not shown).

Statistical Analysis

Representative endomicroscopic images of n=258 different human tissues were evaluated by n=4 different evaluators (surgeons and neuropathologists) and the accuracy was calculated. Astrocytic tumors (I-III) (75%), glioblastomas (100%), ependymomas (75%), epidermoid cyst (50%), schwannomas (100%), meningiomas (100%), brain metastases from lung carcinoma (100%), brain metastases from rectum carcinoma (100%), choroid plexus papillomas (100%), pituitary adenomas (75%) and neurofibromas (100%) were diagnosed with high accuracy. Overall, the average correct detection rate was 88.64%.

To summarize: All tumors were identified with high accuracy. Using CLE neoplastic tissue could be clearly discriminated from non-neoplastic tissue based on cellular and subcellular histomorphology. The performance of CLE on all samples was easy to carry out and overall, good quality images revealing fine histopathological details were obtained. The use of AF in all samples provided satisfactory contrast for endomicroscopic imaging. Furthermore, we demonstrated that neither the fixation process, nor the age of the sample have an effect on CLE examination after topical application of AF (Figure 7).

Discussion

This study was designed to give a first insight into CLE’s potential as a fast and routinely used diagnosis tool for brain and spinal cord lesions. Our *ex vivo* approach demonstrated the usefulness of handheld CLE in the diagnosis of tumors. CLE enabled clear differentiation between neoplastic and non-neoplastic tissue. Moreover, primary brain and spinal tumors, metastases, abscesses and other CNS lesions could be distinguished. CLE was easy to perform and CLE images were comparable with traditional histology as the gold standard.

The decision to perform surgery as a treatment of tumors depends on the location, size, grade and type of tumor as well as the patient’s age. In order to determine the grade and type of a tumor and to further distinguish the tumor from other tissue, traditional histology and frozen sections are routinely performed. Unfortunately, traditional histology is time-consuming and frozen section analysis can lead to incorrect diagnosis due to sampling errors or a poor sample quality. Thus, none of these techniques are ideal for analyzing tumor margins in an ongoing surgery to aid a complete resection. An incomplete resection can result in recurrence of the tumor, whereas a too excessive resection can destroy healthy, vital tissue leading to neurological deficits [18]. On the other hand, CLE permits *in vivo* histological imaging of the entire tissue in real-time and is therefore well suited for tumor margin assessments. The virtual histology of tumors using CLE has already been used for diagnostic purposes in other clinical disciplines, such as gastroenterology, gynecology, urology, otolaryngology and pulmonology [4-10]. Especially in gastroenterology, published data showed an accurate correlation between the confocal images and

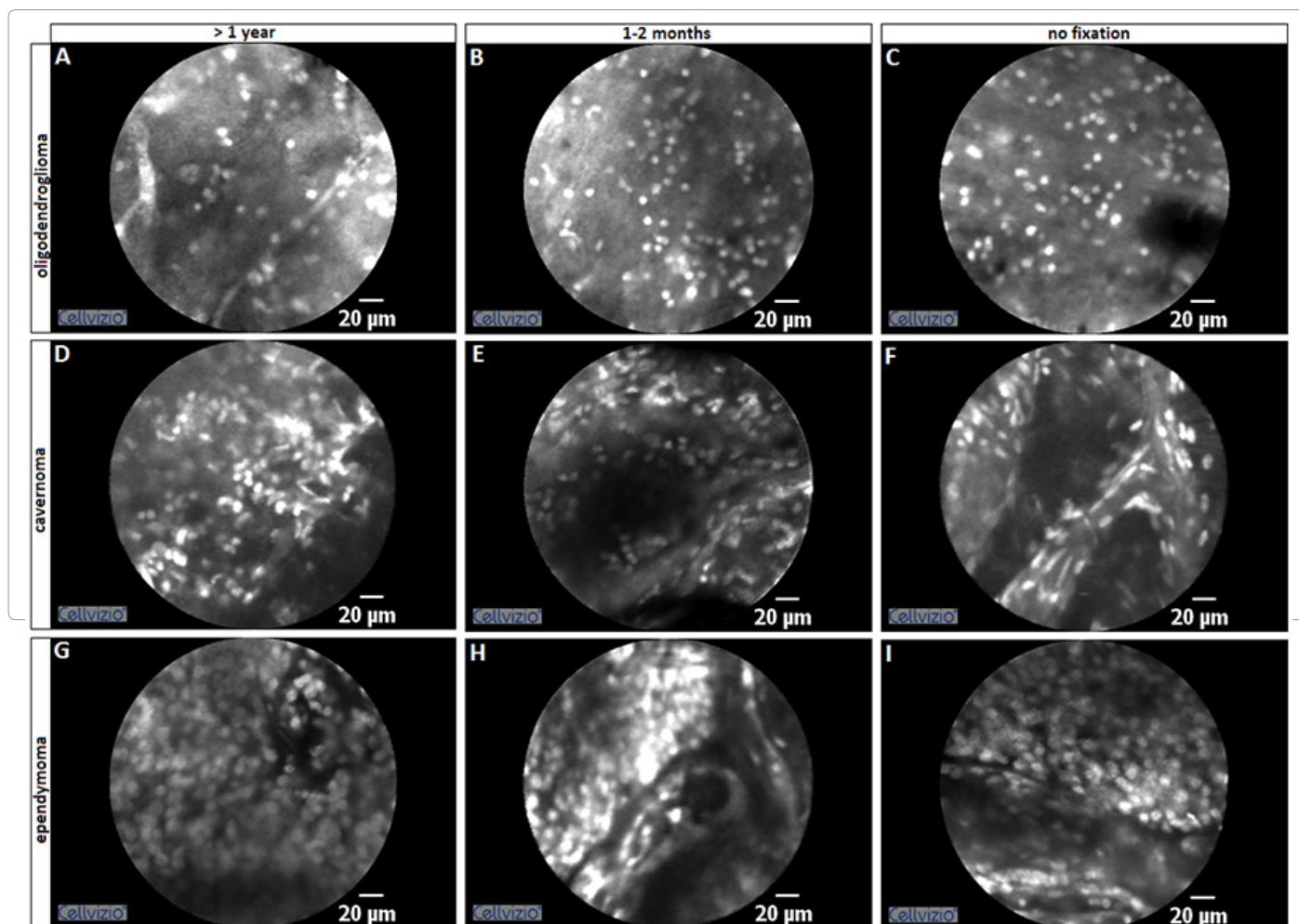


Figure 7: Analyses of tumor samples with AF after fixation with formalin (A, D, G) or without fixation (D, F, I). Oligodendroglioma (A, B, C), cavernoma (D, E, F), and ependymoma (G, H, I) were examined directly after surgery or after fixation in formalin (1 year or 1-2 months ago). Our results show that neither the fixation process, nor the ages of the sample have an effect on CLE examination after topical application of AF. Bars = 20 µm.

conventional histology [4,8]. So far, only a few reports have been published concerning the utilization of CLE in neuro-oncology in either *ex vivo* or *in vivo* human studies [12-15,19]. In particular in this discipline, cellular imaging would be of great importance to avoid injury to healthy, vital tissue. To use CLE for intraoperative diagnosis, the neuropathologist and/or the surgeon need to be familiar with confocal images. They must be able to distinguish between healthy and malignant tissue, between a tumor and other tissue and between the different kinds and grades of tumors to enable ideal patient treatment. For this goal, confocal images of non-neoplastic and 258 brain and spinal cord intra and extra axial located lesions were analyzed, and the features identified on the confocal images were described in detail according to the WHO criteria [1]. Altogether, we examined tumors of neuroepithelial tissue, of the meninges, of cranial and paraspinal nerves, of the hematopoietic system, of the sella region, brain metastases and more seldom CNS lesions and reached an accuracy of 88.64% in identifying the correct tumor.

Of these, gliomas are the most common primary brain tumors and are classified into three main types; astrocytomas (including glioblastoma multiforme), ependymomas, and oligodendrogliomas. Ependymomas and oligodendrogliomas are rare gliomas (2% and 3%, respectively), which are divided into slow (low grade) and fast (high grade) growing types [20]. WHO grade IV astrocytomas are the

most common gliomas found in adults and children [21]. High-grade astrocytomas are fast growing and diffuse infiltrating tumors (WHO grades III and IV). Their infiltrative nature makes a complete resection with the current available equipment impossible due to the inability to distinguish between malignant and healthy tissue at a cellular level [22]. Moreover, the risk of destroying healthy vital tissue is too high [23]. Hence, high resolution imaging at a cellular level could most likely increase the diagnostic yield and survival rate. Especially in the case of gliomas, it was shown that the sooner an intraoperative assessment was made the higher the survival outcome would be [24].

About 1 of 4 brain tumors in adults (33%) is a meningioma [25], which was also the most frequent tumor in our study (28%). Most meningiomas are benign and separable from underlying brain, whereas some infiltrate the brain and make a complete resection challenging (WHO grade III). We examined benign meningiomas (WHO grade I), atypical meningiomas (WHO grade II) and anaplastic meningiomas (WHO grade III). Most of the WHO grades II and III meningiomas yield a high risk of recurrence [26]. Additionally, CLE imaging identified pathological features of pituitary adenomas, hemangioblastomas and schwannomas, which are also frequent benign tumors of the CNS. Generally, benign tumors are slow in growth and have a low tendency to spread. However, they can cause several additional health problems such as headaches, seizures and the disturbance of brain functions.

Furthermore, various diseases such as polycythemia are associated with benign tumors. Pituitary adenomas were shown to cause problems due to a mass effect in the sella resulting from a suppression of the pituitary gland and suprasellar, leading to hypopituitarism or to a complete insufficiency of the pituitary gland [27]. Thus, an early identification and resection of these tumors is important to prevent serious health problems.

In contrast to benign tumors, metastatic tumors are the most common and lethal brain tumors with 98,000-170,000 death cases per year [28]. Most brain metastases are well demarcated from the surrounding tissue and contain histopathological features of the primary tumor. Our approach allowed a precise differentiation between the metastases and healthy tissue. Furthermore, we were able to distinguish between metastasis and abscesses, which was impossible intraoperatively. Previously, a distinction was only possible by means of diffusion tensor imaging, which has its limitations in the differentiation between cystic metastases and abscesses [29]. As a result, the implementation of CLE in neurosurgery has the capability of increasing the diagnostic yield and reducing the risk of false treatment due to easier and more precise tissue identification. The use of CLE would minimize the number of biopsies due to a target “smart” biopsy or an “optical” biopsy, thus reducing the risk of damaging eloquent brain and spinal tissue. Limitation of this study was the use of AF for tissue examination, which is not approved by the food and drug administration (FDA) for *in vivo* human application. Nonetheless, AF can be used as a fast *ex vivo* stain for the immediate diagnosis of biopsies via CLE during surgery. Furthermore, Lee and colleague (2014) [30] demonstrated an anti-tumor activity of AF in cell culture and Shay and colleague [31] its positive effect in slowing tumor progression in mice in the same year. Thus, the *in vivo* human application of AF has to be further analyzed for its clinical safety. Thus, the *in vivo* human application of AF has to be further analyzed for its clinical safety.

On the other hand, 5-aminolaevulinic acid (5-ALA), which is converted in the mitochondria to the endogenous fluorophore protoporphyrin IX (PpIX) and accumulates in neoplastic cells due to the blood-to-brain barrier disruption, is approved by the FDA for surgical purposes in Europe and Asia [32]. 5-ALA is a very useful approach to better detect tumor tissue and achieve gross-total tumor resection due to a higher accumulation of PIX in high-grade gliomas. Unfortunately, low-grade gliomas such as astrocytomas I-III and other tumors do not show PIX fluorescence [32]. Furthermore, CLE (Optiscan PTY., Ltd., 488 nm) examination of 5-ALA induced fluorescence (440/635 nm) could not identify appropriate tumor cells [33]. Hence, this fluorophore is not suitable in tumor detection using CLE. Therefore, fluorescein sodium, indocyanine green, fluorescently labeled antibodies or other dyes should be taken into consideration.

In conclusion, CLE is a useful and reliable tool generating real-time confocal images to identify malignant tumor tissue similar to conventional histology. Our studies have the potential to establish a faster preliminary diagnosis in ongoing surgery as compared to current available methods (frozen section analyses, traditional histology). The presented characteristic cellular and subcellular confocal features of examined tumors could be used to guide future tumor surgery via telemedicine or video transmission in cooperation with the surgeon and neuropathologist, thus making immediate surgical decisions possible. A real-time diagnosis could avoid a second surgery and facilitate a faster treatment. Moreover, CLE could be used to examine tumor margins to enable a more precise and safe resection of tumors. Safe removal without injury to healthy, eloquent tissue is of great importance, since such injury could have disastrous consequences and lead to a loss of

independence for the patient. To achieve this goal, CLE requires further examinations of brain and spinal specimens, a suitable fluorescent dye for clinical trials and intraoperative evaluation.

Acknowledgments

We thank our clinical colleagues at the Medical Hospital in Cologne for their cooperation

Disclosure

The authors report no conflict of interest concerning the materials or methods used in this study or the findings specified in this paper.

References

1. Louis David NOH, Wiestle Otmar D, Cavenee Webster K, Burger Peter C, et al. (2007) The 2007 WHO Classification of Tumours of the Central Nervous System. *Acta Neuropathol* 114: 97-109.
2. Yong RL, Wu T, Mihatov N, Shen MJ, Brown MA, et al. (2014) Residual tumor volume and patient survival following reoperation for recurrent glioblastoma. *Journal of neurosurgery* 121: 802-809.
3. Ajan A, Recht L (2014) Supratentorial low-grade diffuse astrocytoma: medical management. *Semin Oncol* 41: 446-457.
4. Kiesslich R, Burg J, Vieth M, Gnaendiger J, Enders M, et al. (2004) Confocal laser endoscopy for diagnosing intraepithelial neoplasias and colorectal cancer *in vivo*. *Gastroenterology* 127: 706-713.
5. Carlson K, Pavlova I, Collier T, Descour M, Follen M, et al. (2005) Confocal microscopy: imaging cervical precancerous lesions. *Gynecologic oncology* 99: S84-88.
6. Haxel BR, Goetz M, Kiesslich R, Gosepath J (2010) Confocal endomicroscopy: a novel application for imaging of oral and oropharyngeal mucosa in human. *Eur Arch Otorhinolaryngol* 267: 443-448.
7. Lane PM, Lam S, McWilliams A, Leriche JC, Anderson MW, et al. (2009) Confocal fluorescence microendoscopy of bronchial epithelium. *Journal of biomedical optics* 14: 024008.
8. Polglase AL, McLaren WJ, Skinner SA, Kiesslich R, Neurath MF, et al. (2005) A fluorescence confocal endomicroscope for *in vivo* microscopy of the upper- and the lower-GI tract. *Gastrointestinal endoscopy* 62: 686-695.
9. Sonn GA, Jones SN, Tarin TV, Du CB, Mach KE, et al. (2009) Optical biopsy of human bladder neoplasia with *in vivo* confocal laser endomicroscopy. *The Journal of urology* 182: 1299-1305.
10. Tan J, Quinn MA, Pyman JM, Delaney PM, McLaren WJ (2009) Detection of cervical intraepithelial neoplasia *in vivo* using confocal endomicroscopy. *BJOG: an international journal of obstetrics and gynaecology* 116: 1663-1670.
11. Charalampaki P, Javed M, Daali S, Heiroth HJ, Igressa A (2015) Confocal Laser Endomicroscopy for Real-time Histomorphological Diagnosis: Our Clinical Experience With 150 Brain and Spinal Tumor Cases. *Neurosurgery* 62 Suppl 1: 171-176.
12. Foersch S, Heimann A, Ayyad A, Spoden GA, Florin L, et al. (2012) Confocal laser endomicroscopy for diagnosis and histomorphologic imaging of brain tumors *in vivo*. *PLoS one* 7: e41760.
13. Schlosser HG, Suess O, Vajkoczy P, van Landeghem FK, Zeitz M, et al. (2010) Confocal neurolasermicroscopy in human brain - perspectives for neurosurgery on a cellular level (including additional comments to this article). *Central European neurosurgery* 71: 13-19.
14. Snuderl M, Wirth D, Sheth SA, Bourne SK, Kwon CS, et al. (2013) Dye-enhanced multimodal confocal imaging as a novel approach to intraoperative diagnosis of brain tumors. *Brain pathology (Zurich, Switzerland)* 23: 73-81.
15. Whitson WJ, Valdes PA, Harris BT, Paulsen KD, Roberts DW (2011) Confocal microscopy for the histological fluorescence pattern of a recurrent atypical meningioma: case report. *Neurosurgery* 68: E1768-1772; discussion E1772-1763.
16. Wirth D, Snuderl M, Sheth S, Kwon CS, Frosch MP, et al. (2012) Identifying brain neoplasms using dye-enhanced multimodal confocal imaging. *Journal of biomedical optics* 17: 026012.
17. Zülch K (1979) Histological typing of tumours of the central nervous system.
18. Ramakrishna R, Hebb A, Barber J, Rostomily R, Silbergeld D (2015) Outcomes in Reoperated Low-Grade Gliomas. *Neurosurgery* 77: 175-184.

19. Eschbacher J, Martirosyan NL, Nakaji P, Sanai N, Preul MC, et al. (2012) In vivo intraoperative confocal microscopy for real-time histopathological imaging of brain tumors. *Journal of neurosurgery* 116: 854-860.
20. Chamberlain MC (2003) Ependymomas. *Current neurology and neuroscience reports* 3: 193-199.
21. Tofte K, Berger C, Torp SH, Solheim O (2014) The diagnostic properties of frozen sections in suspected intracranial tumors: A study of 578 consecutive cases. *Surg Neurol Int* 5: 170.
22. Kowalczuk A, Macdonald RL, Amidei C, Dohmann G, 3rd, Erickson RK et al. (1997) Quantitative imaging study of extent of surgical resection and prognosis of malignant astrocytomas. *Neurosurgery* 41: 1028-1036; discussion 1036-1028.
23. Duffau H (2014) Preserving quality of life is not incompatible with increasing overall survival in diffuse low-grade glioma patients. *Acta neurochirurgica* 157: 165-167.
24. Sanai N, Berger MS (2012) Recent surgical management of gliomas. *Adv Exp Med Biol* 746: 12-25.
25. Ibebuike K, Ouma J (2014) Demographic profile of patients diagnosed with intracranial meningiomas in two academic hospitals in Johannesburg, South Africa: a 12-month prospective study. *African health sciences* 14: 939-945.
26. Cao X, Hao S, Wu Z, Wang L, Jia G, et al. (2015) Survival rates, prognostic factors and treatment of anaplastic meningiomas. *Journal of clinical neuroscience : official journal of the Neurosurgical Society of Australasia* 22: 828-833.
27. Foppiani L, Ruelle A, Cavazzani P, Del Monte P (2009) Hyperthyroidism unmasked several years after the medical and radiosurgical treatment of an invasive macroprolactinoma inducing hypopituitarism: a case report. *Cases journal* 2: 6449.
28. Nussbaum ES, Djalilian HR, Cho KH, Hall WA (1996) Brain metastases. Histology, multiplicity, surgery, and survival. *Cancer* 78: 1781-1788.
29. Toh CH, Wei KC, Ng SH, Wan YL, Lin CP, et al. (2011) Differentiation of brain abscesses from necrotic glioblastomas and cystic metastatic brain tumors with diffusion tensor imaging. *AJNR American journal of neuroradiology* 32: 1646-1651.
30. Lee CJ, Yue CH, Lin YY, Wu JC, Liu JY (2014) Antitumor activity of acriflavine in human hepatocellular carcinoma cells. *Anticancer research* 34: 3549-3556.
31. Shay JE, Imtiyaz HZ, Sivanand S, Durham AC, Skuli N et al. (2014) Inhibition of hypoxia-inducible factors limits tumor progression in a mouse model of colorectal cancer. *Carcinogenesis* 35: 1067-1077.
32. Stummer W, Pichlmeier U, Meinel T, Wiestler OD, Zanella, et al. (2006) Fluorescence-guided surgery with 5-aminolevulinic acid for resection of malignant glioma: a randomised controlled multicentre phase III trial. *Lancet Oncol* 7: 392-401.
33. Sanai N, Snyder LA, Honea NJ, Coons SW, Eschbacher JM, et al. (2011) Intraoperative confocal microscopy in the visualization of 5-aminolevulinic acid fluorescence in low-grade gliomas. *Journal of neurosurgery* 115: 740-748.

Citation: Samira D, Mehreen J, Ann-Kristin A, Alhadi I, Maximilian L, et al. (2016) Analysis of 258 Different Lesions of the Central Nervous System for Real Time Histopathological Diagnosis Using Confocal Laser Endomicroscopy. *J Mult Scler (Foster City)* 3:169. doi:[10.4172/2376-0389.1000169](https://doi.org/10.4172/2376-0389.1000169)

OMICS International: Publication Benefits & Features

Unique features:

- Increased global visibility of articles through worldwide distribution and indexing
- Showcasing recent research output in a timely and updated manner
- Special issues on the current trends of scientific research

Special features:

- 700+ Open Access Journals
- 50,000+ editorial team
- Rapid review process
- Quality and quick editorial, review and publication processing
- Indexing at major indexing services
- Sharing Option: Social Networking Enabled
- Authors, Reviewers and Editors rewarded with online Scientific Credits
- Better discount for your subsequent articles

Submit your manuscript at: <http://www.omicsonline.org/submission/>